Mathematics and Computers in Simulation 245 (2026) 35–52

Contents lists available at ScienceDirect

Mathematics and Computers in Simulation

journal homepage: www.elsevier.com/locate/matcom

Original articles

Modelling financial contagion and optimal policy design for bank runs and systemic risk

Samuel Asante Gyamerah [a,*], Emmanuel Afrifa [b], Perpetual Andam Boiquaye [c], Nelson Dzupire [d]

[a] Department of Mathematics, Toronto Metropolitan University, Toronto, Canada
[b] African Institute for Mathematical Science, Accra, Ghana
[c] Department of Statistics and Actuarial Science, University of Ghana, Accra, Ghana
[d] Department of Mathematical Sciences, University of Malawi, Zomba, Malawi

ARTICLE INFO

Keywords:
Financial contagion
Bank runs
Epidemiological modelling
Optimal control
Deposit insurance
Systemic risk

ABSTRACT

Bank runs can destabilize individual institutions and, through financial networks, spread into general economic crises. The study explores the interconnection of systemic risk in the banking system, emphasizing interbank networks as the primary means of propagating financial contagion. We propose a compartmental system through which contagion is propagated. The system classifies the banks in the network into six compartments (undistressed, exposed, distressed, liquid, run, and failed states). We capture the dynamics of distress transmission through interbank interactions and depositor behaviours. We derive the basic reproduction number $\mathcal{R}_0$ to characterize the threshold conditions for systemic stability and identify both risk-free and risk-persistent equilibrium points. Through sensitivity experiments, we identify the parameters that exert the strongest influence on contagion dynamics—the contact rate between banks, the level of behavioural compliance, and transition intensities. Building on these insights, we formulate an optimal-control framework that incorporates three forms of intervention: deposit-insurance protection, policies aimed at calming depositors, and targeted liquidity intervention. Using Pontryagin's Maximum Principle, we derive the time paths of these interventions that jointly reduce the spread of distress while keeping regulatory costs manageable. The numerical results highlight the importance of acting early: even a moderate level of deposit-insurance coverage, when implemented at the right moment, substantially dampens the transmission of shocks across the network. The study offers practical guidance for the design of policy tools intended to contain systemic risk in interconnected banking systems.

1. Introduction

The stability of the banking system is one of the most important factors for economic growth and resilience. In the process of increasing globalization, the interconnectedness of financial institutions such as banks, enterprises, and insurance companies has increased considerably [1,2]. Although this interdependence enhances economic efficiency, it exposes the financial system to systemic risks. An example is the risk of bank runs, where a large number of depositors simultaneously withdraw their funds due to concerns about a bank's solvency. Such runs can destabilize individual banks and, through financial networks, spread into general economic crises. Historical events such as the Great Depression and the global financial crisis of 2008 proved how devastating

* Corresponding author.
E-mail address: asante.gyamerah@torontomu.ca (S.A. Gyamerah).

https://doi.org/10.1016/j.matcom.2025.12.023
Received 11 August 2025; Received in revised form 5 December 2025; Accepted 29 December 2025

Available online 3 January 2026

financial contagion could be [3]. Bank runs are local events that can trigger financial contagion, where distress spreads across connected institutions and markets. The Asian financial crisis in the late 1990s also demonstrated how the fragile banking system of interdependent economies could shape a localized disruption into a more globalized crisis. Similarly, in the 2008 financial crisis, the effects of contagion highlighted how close the global banking sector was to collapsing. Thus, these crises have revealed how depositor panic and loss of confidence in financial institutions could amplify systemic risks.

In modern financial systems, characterized by fractional reserve banking and rapid information exchange, the risk of bank runs is even higher. For example, in the 2023 Silicon Valley Bank crisis, adverse online information about the bank's solvency led to a panic among depositors [4]. This resulted in enormous, instantaneous withdrawals sometimes referred to as a "digital bank run". That panic exacerbated the bank's liquidity challenges and eventually caused its collapse. The failure of Silicon Valley Bank in the US in March 2023 sent shockwaves across the banking sector. In response to the incident, four significant banks, namely JPMorgan Chase, Bank of America, Wells Fargo, and Citigroup, altogether lost about USD 52 billion in market value on March 9, 2023 [5]. These events show how important it is to understand the underlying mechanism of bank runs and find strategies to mitigate their cascading effects on the financial system.

Despite the importance of mitigating bank runs, traditional financial models often fail to capture the systemic feedback loops and network effects that drive such events. Liu [6] discusses how the risks of within-bank coordination and cross-bank externalities increase vulnerability, while Peck and Setayesh [7] found that deposit reduction is associated with increased systemic fragility. These works further underline the demand for models that account for both individual depositor behaviours and dynamic distress contagion in the financial system. To bridge this gap, researchers have adapted epidemiological approaches to study financial contagion by borrowing from well-known epidemic compartment models, such as the Susceptible–Infected–Recovered and Susceptible–Infected–Susceptible models. For example, earlier financial contagion models, such as the EDB model of Brandi et al., treated liquidity distress in interbank markets as a unidirectional propagation of funding shortages [8]. That is, banks move from Expose to Distress to Bankrupt under a purely liquidity-driven mechanism on a network of bilateral exposures. While valuable in linking market topology to contagion speed, this model does not incorporate behavioural responses (e.g., depositor runs) or post-intervention recovery channels (e.g., liquidity support or recapitalization). More recently, Chen and Fan extended the SIS-type framework to allow reversibility between "infected" and "susceptible" banks, emphasizing heterogeneous contagion and recovery rates under macroprudential liquidity regulation [9]. However, their model, just like the model of Irakoze et al. [10,11] remained focused on interbank liquidity cycles and does not explicitly capture depositor behaviour. Our six-compartment model (undistressed, exposed, distressed, run, liquid, failed) builds on these foundations by linking market-based contagion (as in Brandi et al. [8]) with behavioural and policy-driven contagion (absent in Chen and Fan [9],Irakoze et al. [10,11]). The additional compartments represent distinct financial realities: "exposed (E)" reflects solvency pressure through asset-value shocks; "distressed (D)" captures funding illiquidity within interbank channels; "run (R)" models depositor panic and coordinated withdrawals; "failed" denotes formal bank failure; and "liquid (L)" represents system-level liquidity restoration through central-bank or fiscal interventions. This model differentiates the transmission channels of distress, those driven by depositor sentiment and liquidity withdrawal, and the subsequent recovery path enabled by policy interventions. This model offers regulators and policymakers a framework for distinguishing solvency contagion from liquidity and confidence contagion and for quantifying how multi-channel controls such as deposit-insurance reinforcement, depositor-calming communication, and liquidity injection jointly mitigate the propagation strength of financial distress within the system. It advances beyond earlier three- or four-compartment formulations by embedding behavioural heterogeneity and policy feedback directly in the dynamic equations of contagion. Associated credit risk spreads in financial networks in a similar way as epidemics spread in biological networks, as both situations involve the spread of negative effects leading to an increasing number of affected individuals/institutions. These studies demonstrate the usefulness of epidemiological models in capturing the cascading effects of financial instability, although there is still a need to incorporate dynamic policy tools effectively.

Deposit insurance has long played a pivotal role in mitigating depositor panic during financial crises. By protecting deposits against the risk of runs or sudden withdrawals, it helps to maintain liquidity within the financial system. Sabourin [12] highlights the importance of adapting stabilization tools such as deposit insurance to address the evolving challenges of modern economies. As a critical mechanism to maintain depositor confidence, deposit insurance is important to curb the spread of financial panic [13]. The COVID-19 pandemic further showed how important robust deposit insurance frameworks are, as increasing economic uncertainty raised the need to make prompt payments to reassure depositors and prevent bank failures [14].

The present study introduces a new approach to mitigating bank runs by developing a deterministic compartmental model that captures the dynamics of financial contagion, which comprises six compartments: undistressed, exposed, distressed, run, failed, and liquid. The model incorporates optimal control strategies for the implementation of targeted interventions: deposit insurance, liquidity injection, and depositor-calming measures to reduce depositor panic and increase stability in the banking system.

The rest of the paper is organized as follows: Section 2 provides the details of the methodology that includes model formulation. The optimal control strategy is discussed in Section 3. Section 4 presents numerical simulations and results, while Section 5 concludes with implications and recommendations for future research.

2. Methodology

2.1. Model formulation

This study uses a deterministic compartmental model to capture the risk contagion in the banking system. It comprises six compartments, namely undistressed, exposed, distressed, run, failed, and liquid compartments. The undistressed compartment, which

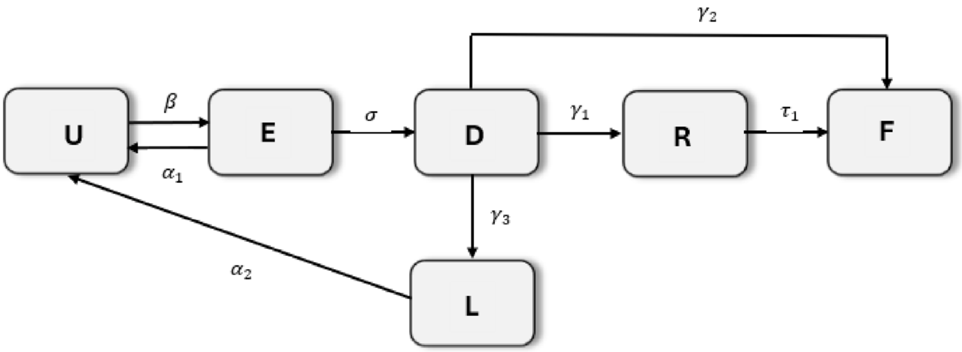

Fig. 1. Dynamics of the risk propagation in the banking sector. Banks transition between Undistressed (U), Exposed (E), Distressed (D), Run (R), Failed (F), and Liquid (L) states.

Table 1
Parameters and their description.

Parameters	Description
β	Contact rate between the undistressed and distressed banks
α_1	The rate at which exposed banks become undistressed
α_2	The rate at which banks in the liquid compartment become undistressed
σ	The rate at which exposed banks become completely distressed
γ_1	The rate at which distressed banks encounter a run state
γ_2	The rate at which distressed banks fail without encountering any run
γ_3	The rate at which distressed banks become liquid after effective risk management
τ_1	The rate at which banks in the run compartment fail

represents banks with no risks, is denoted by U; the exposed compartment includes banks that have been exposed to risks in the banking system and is denoted by E; and the banks currently at risk are referred to as distressed banks, denoted by D. The run compartment is represented by R and consists of banks that are experiencing panic withdrawals due to concerns about the bank's solvency; banks that have failed due to financial distress move to the failed compartment, which is represented by F; the liquid compartment, denoted by L, represents banks that have successfully managed risks, restoring liquidity and stability; and N denotes the total number of banks in the system. The model assumes a force of contagion (distress transmission) given by $(1-\delta)\beta U D$, where δ is the fraction of banks that practice effective risk management and compliance. The flowchart demonstrating the propagation of the risk in the banking system is shown in Fig. 1, and the parameters therein are explained in Table 1.

2.1.1. Model assumptions

- The number of banks in the system remain fixed.
- There is a homogeneous mixing of the banks in the system.
- Transmission is only from bank to bank.
- Exposed banks can become undistressed again after effective risk management without progressing to the distressed state.

The system of non-linear differential equations that model the dynamics is given below:

$$\begin{cases} \frac{dU}{dt} &= \alpha_1 E + \alpha_2 L - (1-\delta)\beta U D, \\ \frac{dE}{dt} &= (1-\delta)\beta U D - (\alpha_1 + \sigma)E, \\ \frac{dD}{dt} &= \sigma E - (\gamma_1 + \gamma_2 + \gamma_3)D, \\ \frac{dR}{dt} &= \gamma_1 D - \tau_1 R, \\ \frac{dF}{dt} &= \gamma_2 D + \tau_1 R, \\ \frac{dL}{dt} &= \gamma_3 D - \alpha_2 L, \end{cases} \tag{1}$$

subject to the initial conditions,

$$U > 0, E \geq 0, D \geq 0, R \geq 0, F \geq 0, L \geq 0.$$

The total number of banks N is given by,

$$N = U + E + D + R + F + L. \tag{2}$$

2.2. Boundedness and positivity

In this section, we establish that the proposed compartmental model adheres to the structural constraints of a closed financial system.

Lemma 2.1. *The system (Equation (1)) has a positively invariant and bounded solution set* $\{U, E, D, R, F, L\}$ *in the feasibility region,*

$$\Omega = \{(U, E, D, R, F, L) \in \mathbb{R}^6 | U + E + D + R + F + L \leq N_0\},$$

for non-negative initial conditions.

Proof. Let $\theta(x)$ be defined by as

$$\{x(t) = 0 | x \in (U, E, D, R, F, L) \text{ and } (U, E, D, R, F, L) \in \mathbb{R}^6 \geq 0\}.$$

It implies

$$\begin{aligned}
\left.\frac{dU}{dt}\right|_{\theta(U)} &= \alpha_1 E + \alpha_2 L \geq 0,\\
\left.\frac{dE}{dt}\right|_{\theta(E)} &= (1-\delta)\beta U D \geq 0,\\
\left.\frac{dD}{dt}\right|_{\theta(D)} &= \sigma E \geq 0,\\
\left.\frac{dR}{dt}\right|_{\theta(R)} &= \gamma_1 D \geq 0,\\
\left.\frac{dF}{dt}\right|_{\theta(F)} &= \gamma_2 D + \tau_1 R \geq 0,\\
\left.\frac{dL}{dt}\right|_{\theta(L)} &= \gamma_3 D \geq 0.
\end{aligned}$$

That is, for any non-negative initial conditions, the solution set will always be non-negative. This completes the first part of the lemma.

From Eq. (2), we have that

$$\begin{aligned}
&\frac{dN}{dt} = \frac{dU}{dt} + \frac{dE}{dt} + \frac{dD}{dt} + \frac{dR}{dt} + \frac{dF}{dt} + \frac{dL}{dt} = 0,\\
\implies &N(t) = N_0,
\end{aligned}$$

where N_0 is a constant. That is, the total number of financial institutions is fixed over time. This reflects a practical assumption in short-term contagion modelling where no new banks are introduced to the financial network during the period of the analysis.

It implies,

$$0 \geq x \geq N_0, \forall\ x \in (U, E, D, R, F, L).$$

Hence, the system is indeed bounded and positively invariant, preserving the economic interpretability of the model. □

2.3. Risk-free equilibrium point, RFE

We analyse the steady-state behaviour of the system in the absence of financial contagion. We define the risk-free equilibrium point as the state where no banks are under distress. To determine the equilibrium point, we equate the right-hand side of the system in Eq. (1) to zero. That is,

$$\alpha_1 E + \alpha_2 L - (1-\delta)\beta U D = 0, \tag{3}$$

$$(1-\delta)\beta U D - (\alpha_1 + \sigma)E = 0, \tag{4}$$

$$\sigma E - (\gamma_1 + \gamma_2 + \gamma_3)D = 0, \tag{5}$$

$$\gamma_1 D - \tau_1 R = 0, \tag{6}$$

$$\gamma_3 D - \alpha_2 L = 0. \tag{7}$$

We neglect the fifth equation of Eq. (1) since it does not explicitly appear in the model equations. At the risk-free equilibrium point, all the risk compartments are zero (i.e., $E = D = 0$). Consequentially, we have $R = 0$, and $L = 0$. We make use of Eq. (2) to find the value for U.

$$\begin{aligned}
&N = U + 0 + 0 + 0 + 0,\\
\implies &U = N.
\end{aligned}$$

Representing the risk-free equilibrium point with κ, we have that,

$$\kappa = (U^*, E^*, D^*, R^*, L^*) = (N, 0, 0, 0, 0).$$

This represents a healthy financial system where all banks are solvent and undisturbed by systemic risk. The risk-free equilibrium provides a benchmark against which the dynamics of contagion and the effectiveness of intervention strategies can be evaluated.

After establishing the risk-free equilibrium, it is important to determine whether it remains stable or becomes unstable. To assess the risk of contagion spreading within the financial network, we calculate the basic reproduction number (R_0) which measures the expected number of newly distressed banks generated by a single distressed bank in an otherwise stable system.

2.4. Basic reproductive number, $\mathcal{R}_0$

The basic reproductive number is the number of secondary risks that can be caused by a single distressed bank in a completely susceptible system. In essence, it gives a measure of how many banks will be affected by the risk given a single distressed bank in the system. We use the next generation matrix (NGM) approach to derive the expression for $\mathcal{R}_0$. With this approach, $\mathcal{R}_0$ is given as the spectral radius of the NGM. That is,

$$\mathbb{R}_0 = \max\{\lambda_i\},$$

where λ_i's are the eigenvalues of the NGM. We consider only the risk compartment,

$$\frac{dE}{dt} = (1-\delta)\beta U D - (\alpha_1 + \sigma)E,$$
$$\frac{dD}{dt} = \sigma E - (\gamma_1 + \gamma_2 + \gamma_3)D.$$

The vector of new risks, $\mathcal{F}$ is

$$\mathcal{F} = \begin{bmatrix} (1-\delta)\beta U D \\ 0 \end{bmatrix}; F = \begin{bmatrix} \frac{\partial \mathcal{F}_1}{\partial E} & \frac{\partial \mathcal{F}_1}{\partial D} \\ \frac{\partial \mathcal{F}_2}{\partial E} & \frac{\partial \mathcal{F}_2}{\partial E} \end{bmatrix} = \begin{bmatrix} 0 & (1-\delta)\beta U \\ 0 & 0 \end{bmatrix}; F(\kappa) = \begin{bmatrix} 0 & (1-\delta)\beta N \\ 0 & 0 \end{bmatrix}.$$

The vector of transitional risks (risks propagating to other compartments), $\mathcal{V}$ is also given by,

$$\mathcal{V} = \begin{bmatrix} (\alpha_1 E) \\ (\gamma_1+\gamma_2+\gamma_3)D - \sigma E \end{bmatrix}; V = \begin{bmatrix} \frac{\partial \mathcal{V}_1}{\partial E} & \frac{\partial \mathcal{V}_1}{\partial D} \\ \frac{\partial \mathcal{V}_2}{\partial E} & \frac{\partial \mathcal{V}_2}{\partial E} \end{bmatrix} = \begin{bmatrix} (\alpha_1+\sigma) & 0 \\ -\sigma & (\gamma_1+\gamma_2+\gamma_3) \end{bmatrix};$$

$$V^{-1} = \begin{bmatrix} \frac{1}{\alpha_1+\sigma} & 0 \\ \frac{\sigma}{(\alpha_1+\sigma)(\gamma_1+\gamma_2+\gamma_3)} & \frac{1}{\gamma_1+\gamma_2+\gamma_3} \end{bmatrix}.$$

The next generation matrix is defined as

$$FV^{-1} = \begin{bmatrix} 0 & (1-\delta)\beta N \\ 0 & 0 \end{bmatrix} \begin{bmatrix} \frac{1}{\alpha_1+\sigma} & 0 \\ \frac{\sigma}{(\alpha_1+\sigma)(\gamma_1+\gamma_2+\gamma_3)} & \frac{1}{\gamma_1+\gamma_2+\gamma_3} \end{bmatrix} = \begin{bmatrix} \frac{(1-\delta)\beta\sigma N}{(\alpha_1+\sigma)(\gamma_1+\gamma_2+\gamma_3)} & \frac{(1-\delta)\beta N}{(\gamma_1+\gamma_2+\gamma_3)} \\ 0 & 0 \end{bmatrix}.$$

$$|FV^{-1} - \lambda I| = \begin{vmatrix} \frac{(1-\delta)\beta\sigma N}{(\alpha_1+\sigma)(\gamma_1+\gamma_2+\gamma_3)} - \lambda & \frac{(1-\delta)\beta N}{(\gamma_1+\gamma_2+\gamma_3)} \\ 0 & -\lambda \end{vmatrix} = 0,$$

$$\lambda_1 = 0,$$
$$\lambda_2 = \frac{(1-\delta)\beta\sigma N}{(\alpha_1+\sigma)(\gamma_1+\gamma_2+\gamma_3)}.$$

By definition,

$$\mathcal{R}_0 = \frac{(1-\delta)\beta\sigma N}{(\alpha_1+\sigma)(\gamma_1+\gamma_2+\gamma_3)}.$$

Fig. 2 captures the temporal evolution of different states in a financial network during a systemic shock and is modelled using an epidemiological model. The curve labelled U (Undistressed) indicates a reduced number of solvent banks with no exposure to market panic or liquidity pressures. As panic spreads (similar to a contagious disease), banks move from a state of Undistress (U) into the Expose (E) state, which represents banking institutions that are vulnerable due to interbank linkages or public rumours but are not yet in distress. Banks in the Exposed state can transition into the D (Distressed) state, where liquidity problems become more pronounced, often due to funding withdrawals or deteriorating asset values. This state reflects the decline in trust seen during actual crises, such as the financial crisis of 2008. The number most likely peaks in R (Run) banks, marking a tipping point where depositor panic triggers mass withdrawals, which is when financial contagion becomes more severe. Some institutions that are unable to recover end up in the F (Failed) compartment, which represents forced closures or defaults. The other banks regain solvency and move into the L (Liquid) compartment through recapitalization or government interventions, such as deposit insurance or liquidity

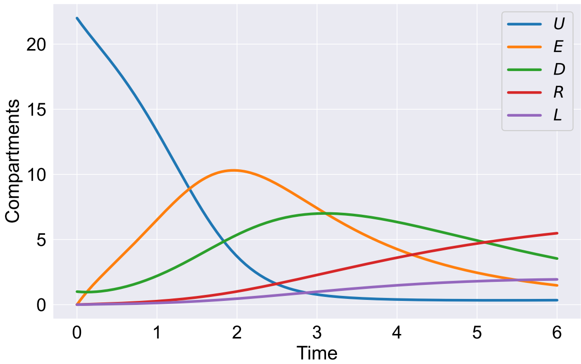

Fig. 2. Temporal dynamics of banking states during contagion. $U(t)$ denotes solvent banks, $E(t)$ exposed banks, $D(t)$ distressed banks, $R(t)$ banks under run pressure, $F(t)$ failed banks, and $L(t)$ liquid or recovered banks.

injections. From a regulatory standpoint, this dynamic shows how early interventions (particularly in the E and D stages) are crucial for containing systemic risk in the banking system. Fig. 2 shows the need for proactive measures to stabilize the banking systems before distress cascades through the entire system.

2.5. Risk-persistent equilibrium point

Contrary to the risk-free equilibrium point, we now derive the risk-persistent equilibrium point, which characterizes the long-run state of the financial system when distress remains endemic. This equilibrium occurs when the system settles into a non-zero level of financial distress, meaning that banks persist in the exposed, distressed, or liquid compartments over time.

This equilibrium point exists when the risk is present in the banking system. From Eq. (5),

$$E = \frac{(\gamma_1 + \gamma_2 + \gamma_3)D}{\sigma}. \tag{8}$$

Substituting Eq. (8) into Eq. (4) yields,

$$(1-\delta)\beta U D - (\alpha_1 + \sigma)\left[\frac{(\gamma_1 + \gamma_2 + \gamma_3)D}{\sigma}\right] = 0.$$

For the system to have an endemic equilibrium point, $D \neq 0$, which implies,

$$U = \frac{(\alpha_1 + \sigma)(\gamma_1 + \gamma_2 + \gamma_3)}{\sigma(1-\delta)\beta} = \frac{N_0}{\mathcal{R}_0}. \tag{9}$$

Substituting Eq. (8) and Eq. (9) into Eq. (3) gives,

$$L = \frac{1}{\alpha_2}(\gamma_1 + \gamma_2 + \gamma_3)D.$$

From Eq. (6),

$$R = \frac{\gamma_1}{\tau_1}D.$$

Let $D^* = D_0 \neq 0$. Hence the risk-persistent equilibrium point,

$$\kappa_p = (U^*, E^*, D^*, R^*, L^*) = \left(\frac{N_0}{\mathcal{R}_0}, \frac{(\gamma_1 + \gamma_2 + \gamma_3)}{\sigma}D_0, D_0, \frac{\gamma_1}{\tau_1}D_0, \frac{1}{\alpha_2}(\gamma_1 + \gamma_2 + \gamma_3)D_0\right),$$

where $D_0 > 0$ is the equilibrium level of distressed banks. The failed compartment F is not included explicitly in this steady-state formulation, as its accumulation is treated as an absorbing state and does not feed back into the other compartments under this model structure.

2.6. Local stability analysis

To assess the resilience of the financial system to perturbations around the equilibrium points, we perform a local stability analysis of both the risk-free equilibrium and the risk-persistent equilibrium. This allows us to determine whether small shocks will die out over time or amplify into systemic crises. Using Eq. (3) - Equation (7), we have our Jacobian matrix for the system (1) as

$$\mathcal{J}=\begin{bmatrix} -(1-\delta)\beta D & \alpha_1 & -(1-\delta)\beta U & 0 & \alpha_2 \\ (1-\delta)\beta D & -(\alpha_1+\sigma) & (1-\delta)\beta U & 0 & 0 \\ 0 & \sigma & -(\gamma_1+\gamma_2+\gamma_3) & 0 & 0 \\ 0 & 0 & \gamma_1 & -\tau_1 & 0 \\ 0 & 0 & \gamma_3 & 0 & -\alpha_2 \end{bmatrix} \tag{10}$$

2.6.1. Local stability analysis of risk-free equilibrium point

We first evaluate the local stability of the risk-free equilibrium $\kappa_0=(N_0,0,0,0,0)$, where all banks are undistressed.

Lemma 2.2. *The risk-free equilibrium point is locally stable if $\mathcal{R}_0<1$ and unstable if $\mathcal{R}_0>1$.*

Proof. The Jacobian matrix (Equation (10)) evaluated at the risk-free equilibrium point gives,

$$\mathcal{J}(\kappa)=\begin{bmatrix} 0 & \alpha_1 & -(1-\delta)\beta N & 0 & \alpha_2 \\ 0 & -(\alpha_1+\sigma) & (1-\delta)\beta N & 0 & 0 \\ 0 & \sigma & -(\gamma_1+\gamma_2+\gamma_3) & 0 & 0 \\ 0 & 0 & \gamma_1 & -\tau_1 & 0 \\ 0 & 0 & \gamma_3 & 0 & -\alpha_2 \end{bmatrix}$$

Let $a_1=(1-\delta)\beta N$, $a_2=\alpha_1+\sigma$, and $a_3=\gamma_1+\gamma_2+\gamma_3$. Thus, $\mathcal{J}(\kappa)$ becomes,

$$\mathcal{J}(\kappa)=\begin{bmatrix} 0 & \alpha_1 & -a_1 & 0 & \alpha_2 \\ 0 & -a_2 & a_1 & 0 & 0 \\ 0 & \sigma & -a_3 & 0 & 0 \\ 0 & 0 & \gamma_1 & -\tau_1 & 0 \\ 0 & 0 & \gamma_3 & 0 & -\alpha_2 \end{bmatrix} \tag{11}$$

To find the eigenvalues of Eq. (11), we set $\det(\mathcal{J}(k)-\lambda I)$ to zero, where I denotes the 5×5 identity matrix.

$$|\mathcal{J}(k)-\lambda I|=\begin{vmatrix} -\lambda & \alpha_1 & -a_1 & 0 & \alpha_2 \\ 0 & -a_2-\lambda & a_1 & 0 & 0 \\ 0 & \sigma & -a_3-\lambda & 0 & 0 \\ 0 & 0 & \gamma_1 & -\tau_1-\lambda & 0 \\ 0 & 0 & \gamma_3 & 0 & -\alpha_2-\lambda \end{vmatrix}=0,$$

$$=-\lambda(-\tau_1-\lambda)(-\alpha_2-\lambda)[\lambda^2+(a_2+a-3)\lambda+a_2a_3-a_1\sigma]=0.$$

It implies,

$$\lambda_1=0$$
$$\lambda_2=-\tau_1$$
$$\lambda_3=-\alpha_2$$
$$\lambda_{4,5}=\frac{-(a_2+a_3)\pm\sqrt{(a_2+a_3)^2-4(a_2a_3-a_1\sigma)}}{2}.$$

For the system to be stable,

$$a_1\sigma<a_2a_3.$$

That is,

$$\frac{(1-\delta)\beta\sigma N}{(\alpha_1+\sigma)(\gamma_1+\gamma_2+\gamma_3)}<1,$$
$$\implies \quad \mathcal{R}_0<1.$$

Thus, the risk-free equilibrium is locally asymptotically stable when $\mathcal{R}_0<1$, indicating that contagion does not occur in a perfectly healthy banking system. However, if $\mathcal{R}_0>1$, small shocks might spread and destabilize the system. □

2.6.2. Local stability analysis of risk-persistent equilibrium point

We examine the risk-persistent equilibrium κ_p derived in Section 2.5.

Lemma 2.3. *The risk-persistent equilibrium point is locally asympototically stable if* $\mathcal{R}_0 > \frac{N(\delta-1)\beta}{\alpha_1+\alpha_2}$.

Proof. Substituting the risk-persistent equilibrium point, κ_p into Eq. (10), we get,

$$\mathcal{J}(\kappa_p) = \begin{bmatrix} -(1-\delta)\beta D_0 & \alpha_1 & -\frac{(1-\delta)\beta N}{\mathcal{R}_0} & 0 & \alpha_2 \\ (1-\delta)\beta D_0 & -(\alpha_1+\sigma) & \frac{(1-\delta)\beta N}{\mathcal{R}_0} & 0 & 0 \\ 0 & \sigma & -(\gamma_1+\gamma_2+\gamma_3) & 0 & 0 \\ 0 & 0 & \gamma_1 & -\tau_1 & 0 \\ 0 & 0 & \gamma_3 & 0 & -\alpha_2 \end{bmatrix} \tag{12}$$

Using Proposition 2.1 (corollary of Gershgorin Circle Theorem) by Adom-Konadu et al. [15] and a similar approach by Bejarano et al. [16], we have that, Given an nxn Jacobian matrix of a dynamical system, if the diagonal entries, $J_{ii}, i = 1, \dots, n$ of J satisfy

$$J_{ii} < -R_i,$$

where

$$R_i = \sum_{j=1, j\neq i}^{n} |J_{ij}|, i = 1, \dots, n,$$

then the eigenvalues of J have negative real parts.

Applying this to our system, the eigenvalues of Eq. (12) will have negative real parts if the following inequalities are satisfied:

$$(1-\delta)\beta D_0 > \alpha_1 + \alpha_2 + \frac{(1-\delta)\beta N}{\mathcal{R}_0}, \tag{13a}$$

$$(\alpha_1+\sigma) > (1-\delta)\beta D_0 + \frac{(1-\delta)\beta N}{\mathcal{R}_0}, \tag{13b}$$

$$(\gamma_1+\gamma_2+\gamma_3) > \sigma, \tag{13c}$$

$$\tau_1 > \gamma_1, \tag{iv}$$

$$\alpha_2 > \gamma_3. \tag{v}$$

Dividing Equation (13b) by $(\alpha_1+\sigma)$ and Eq. (13c) by σ, we get,

$$1 > \frac{1}{\alpha_1+\sigma}\left[(1-\delta)\beta D_0 + \frac{(1-\delta)\beta N}{\mathcal{R}_0}\right], \tag{13}$$

$$\frac{\gamma_1+\gamma_2+\gamma_3}{\sigma} > 1. \tag{14}$$

Putting Equation (13) and Eq. (14) together,

$$\frac{\gamma_1+\gamma_2+\gamma_3}{\sigma} > \frac{1}{\alpha_1+\sigma}\left[(1-\delta)\beta D_0 + \frac{(1-\delta)\beta N}{\mathcal{R}_0}\right],$$

$$1 > \frac{\mathcal{R}_0}{N}\left[D_0 + \frac{N}{\mathcal{R}_0}\right] \tag{15}$$

From Equation (13a),

$$D_0 - \frac{(\alpha_1+\alpha_2)}{(1-\delta)\beta} > \frac{N}{\mathcal{R}_0} \tag{16}$$

Multiplying Equation (15) and Eq. (16) gives,

$$\mathcal{R}_0 > \frac{N(\delta-1)\beta}{(\alpha_1+\alpha_2)} \tag{17}$$

Hence, the risk-persistent equilibrium point is locally asymptotically stable if the inequality in Eq. (17) holds. This scenario can be interpreted as a banking system in which financial contagion persists endemically, maintaining a steady-state level of systemic risk, despite the presence of some risk mitigation mechanisms. □

2.7. Sensitivity analysis

To understand the influence of model parameters on the propagation of financial distress, we conduct a sensitivity analysis of the basic reproduction number $\mathcal{R}_0$. In this study, we utilize the forward sensitivity index defined as

$$C^{p}_{\mathcal{R}_0} = \frac{\partial \mathcal{R}_0}{\partial p} \cdot \frac{p}{\mathcal{R}_0},$$

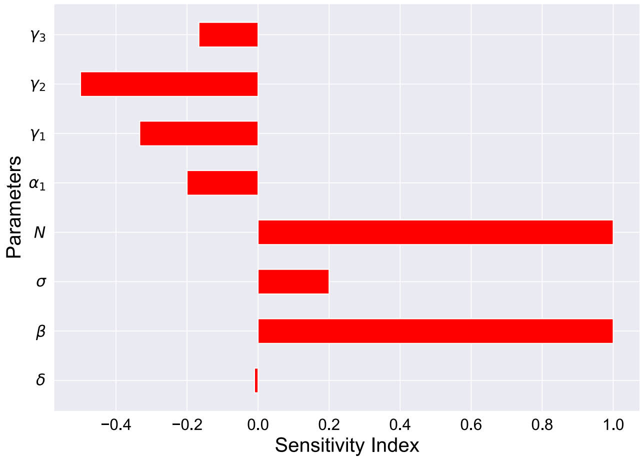

Fig. 3. Sensitivity analysis of parameters influencing R_0. Bars represent the relative impact of each parameter on the contagion potential within the banking system.

where p denotes the parameter of interest. The sensitivity index measures the relative change in $\mathcal{R}_0$ in response to a relative change in parameter p, and thus provides insight into which parameters most strongly influence contagion dynamics. The sensitivity indices for the parameters in this study are as follows:

- Risk management compliance rate(δ):

$$C_{\mathcal{R}_0}^{\delta} = -\frac{\beta\sigma N}{(\alpha_1+\sigma)(\gamma_1+\gamma_2+\gamma_3)} \cdot \frac{\delta(\alpha_1+\sigma)(\gamma_1+\gamma_2+\gamma_3)}{(1-\delta)\beta\sigma N} = -\frac{\delta}{1-\delta}$$

  An increase in effective compliance significantly reduces $\mathcal{R}_0$, confirming its role in suppressing contagion.
- Contact rate (β) and bank population size (N_0)

$$C_{\mathcal{R}_0}^{\beta} = \frac{(1-\delta)\sigma N}{(\alpha_1+\sigma)(\gamma_1+\gamma_2+\gamma_3)} \cdot \frac{\beta(\alpha_1+\sigma)(\gamma_1+\gamma_2+\gamma_3)}{(1-\delta)\beta\sigma N} = 1$$

  These parameter scale $\mathcal{R}_0$ linearly. Higher interbank exposure or system size amplifies the spread of distress.
- Distress progression rate ($sigma$)

$$C_{\mathcal{R}_0}^{\sigma} = \frac{\alpha_1(1-\delta)\beta N}{(\alpha_1+\sigma)(\gamma_1+\gamma_2+\gamma_3)} \cdot \frac{\sigma(\alpha_1+\sigma)(\gamma_1+\gamma_2+\gamma_3)}{(1-\delta)\beta\sigma N} = \frac{\alpha_1}{\alpha_1+\sigma}$$

  The sensitivity ranges from 0 to 1, indicating that its effect is noticeable but not dominant and depends largely on how quickly banks move from the exposed state into distress.
- Initial number of banks (N_0)

$$C_{\mathcal{R}_0}^{N_0} = \frac{(1-\delta)\beta\sigma}{(\alpha_1+\sigma)(\gamma_1+\gamma_2+\gamma_3)} \cdot \frac{N(\alpha_1+\sigma)(\gamma_1+\gamma_2+\gamma_3)}{(1-\delta)\beta\sigma N} = 1$$

  An increase in the initial number of banks increases the rate of financial contagion.
- Recovery rate from exposure (α_1)

$$C_{\mathcal{R}_0}^{\alpha_1} = -\frac{(1-\delta)\beta\sigma(\gamma_1+\gamma_2+\gamma_3)}{[(\alpha_1+\sigma)(\gamma_1+\gamma_2+\gamma_3)]^2} \cdot \frac{\alpha_1(\alpha_1+\sigma)(\gamma_1+\gamma_2+\gamma_3)}{(1-\delta)\beta\sigma N} = -\frac{\alpha_1}{\alpha_1+\sigma}$$

  A higher α_1 directly reduces the risk of banks becoming fully distressed, lowering $\mathcal{R}_0$.
- Transition rates from distress ($\gamma_1, \gamma_2, \gamma_3$)

$$C_{\mathcal{R}_0}^{\gamma_i} = -\frac{(1-\delta)\beta\sigma N(\alpha_1+\sigma)}{[(\alpha_1+\sigma)(\gamma_1+\gamma_2+\gamma_3)]^2} \cdot \frac{\gamma_i(\alpha_1+\sigma)(\gamma_1+\gamma_2+\gamma_3)}{(1-\delta)\beta\sigma N} = -\frac{\gamma_i}{\gamma_1+\gamma_2+\gamma_3}, \quad i = 1, 2, 3.$$

  Each of these parameters contributes to lowering $\mathcal{R}_0$ with proportional influence.

These findings guide both regulatory design and intervention priorities. In particular, enhancing compliance measures (δ) and strengthening mechanisms that enable distressed banks to exit distress (via liquidation or failure resolution) are most effective in lowering systemic risk. In Fig. 3, we present the sensitivity analysis of parameters influencing R_0.

3. Optimal control analysis

To help curb the spread of the contagion in the banking system, we formulate an optimal control framework that introduces dynamic intervention strategies. We design these strategies to reduce the number of banks in the exposed, distressed, and run compartments, thereby mitigating systemic risk. The analysis considers three control variables representing common regulatory tools:

- u_1 = intensity of deposit insurance mechanisms,
- u_2 = depositor-calming policies, such as communication strategies or partial withdrawal limitations,
- u_3 = Liquidity Injection, including central bank or fiscal support aimed at stabilizing distressed banks.

u_1 is the combined effect of the effective coverage ratio and payout, and payout efficiency. A higher value of u_1 reflects quicker payouts and wider deposit coverage by the insurance scheme. This reassurance minimizes the fear of potential losses and slows the shift from the Undistressed (U) to Exposed (E) state. u_2 represents policy actions that aim to calm depositors and restore confidence, such as public assurances from central banks, clear communication about bank stability, or temporary limits on withdrawals designed to moderate panic-driven withdrawals. In the model, u_2 acts primarily on the $D \to R$ transition, lowering the contagion rate of behavioural runs by influencing depositor sentiment. u_3 captures emergency liquidity provision and recapitalization programs by the central bank or fiscal authorities. It captures central bank and government interventions aimed at restoring liquidity to distressed banks, such as emergency loans, liquidity facilities, or direct recapitalizations. u_1 mitigates solvency perceptions, u_2 manages behavioural contagion, and u_3 restores system liquidity.

The aim is to determine the best set of controls alongside their control profile for minimizing the number of banks in the exposed, distressed, and run compartments. Suppose $x'(t) = f(x(t))$ is the system of differential equations governing the contagion in the banking system with initial conditions $x(0) = x_0 \in \mathbb{R}^n$. Let $u_i(t) \in \mathcal{U}$ represent the control variables, where $\mathcal{U}$ is the admissible control set given as $\{(u_1, u_2, u_3) | 0 \le u_i \le 1, i = 1,2,3$ and Lebesgue measurable on$[0,1]\}$ and $t_0 \le t \le t_f$ denote the time interval. The objective functional is given as

$$\mathcal{J}(u_1,u_2,u_3) = \int_{t_0}^{t_f} \left[E(t) + D(t) + R(t) + \frac{B_1}{2}u_1^2 + \frac{B_2}{2}u_2^2 + \frac{B_3}{2}u_3^2 \right] dt, \tag{18}$$

subject to

$$\begin{cases} \frac{dU}{dt} &= \alpha_1 E + \alpha_2 L - (1-(\delta+u_1))\beta U D, \\ \frac{dE}{dt} &= (1-(\delta+u_1))\beta U D - (\alpha_1+\sigma)E, \\ \frac{dD}{dt} &= \sigma E - (\gamma_2 + u_2 + u_3)D, \\ \frac{dR}{dt} &= u_2 D - \tau_1 R, \\ \frac{dL}{dt} &= u_3 D - \alpha_2 L, \end{cases} \tag{19}$$

with initial conditions

$$U(t) > 0, E(t) \ge 0, D(t) \ge 0, R(t) \ge 0, L(t) \ge 0.$$

The constants, $B_i, i = 1,2,3$ are non-negative (i.e. $B_i > 0$) and they denote the importance of the controls u_1, u_2 and u_3. The controls, u_i are non-linear with a quadratic form. The quadratic term implies that too much of the control is implemented [17]. The half term reduces the effect of the control. The objective is to find the set of controls, u^* such that

$$\mathcal{J}(u_1^*, u_2^*, u_3^*) = \min J(u_1,u_2,u_3).$$

The optimal control problem exists if the Fillipov–Cesari theorem is satisfied [18]. It states that for the optimal control problem to exist, the following conditions must be satisfied:

1. The state and control sets must be non empty.
2. The state and control variables must be closed and bounded.
3. The integrand of $\mathcal{J}$ must be convex with respect to the $u_i(t)$.
4. The system must be bounded by a linear function in the state and control variables.

By definition of the admissible control set, it is closed and bounded, as are the state variables of the system. We show that the integral of the objective function is convex by finding the Hessian matrix. It is given by

$$\begin{bmatrix} B_1 & 0 & 0 \\ 0 & B_2 & 0 \\ 0 & 0 & B_3 \end{bmatrix}.$$

Since we have $B_i > 0$ for $i = 1,2,3$, the Hessian is positive definite, which implies that the integrand of $\mathcal{J}$ is strictly convex.

Using Pontryagin's Maximum Principle [17,19], we transform Equation (18) and Eq. (19) into a problem of minimizing the Hamiltonian, $\mathcal{H}$, pointwise with respect to the admissible controls, u_1, u_2 and u_3.

$$\mathcal{H} = E(t) + D(t) + R(t) + \frac{A_1}{2}u_1^2 + \frac{B_2}{2}u_2^2 + \frac{B_3}{2}u_3^2$$

$$
\begin{aligned}
&+ \lambda_1[\alpha_1 E + \alpha_2 L - (1-(\delta+u_1))\beta U D] \\
&+ \lambda_2[(1-(\delta+u_1))\beta U D - (\alpha_1+\sigma)E] \\
&+ \lambda_3[\sigma E - (\gamma_2 + u_2 + u_3)D] \\
&+ \lambda_4[u_2 D - \tau_1 R] \\
&+ \lambda_5[u_3 D - \alpha_2 L].
\end{aligned}
$$

There exists the adjoint function $\lambda_i, i = 1, \dots, 5$ such that

$$
\begin{aligned}
\frac{d\lambda_1}{dt} &= -\frac{\partial \mathcal{H}}{\partial U} = \lambda_1(1-(\delta+u_1))\beta D + \lambda_2(1-(\delta+u_1)\beta D) \\
\frac{d\lambda_2}{dt} &= -\frac{\partial \mathcal{H}}{\partial E} = \lambda_2(\alpha_1+\sigma) - \lambda_3\sigma - \lambda_1\alpha_1 - 1 \\
\frac{d\lambda_3}{dt} &= -\frac{\partial \mathcal{H}}{\partial D} = \lambda_1[(1-(\delta+u_1))\beta U] - \lambda_2[(1-(\delta+u_1))\beta U] + \lambda_3(\gamma_1+u_2+u_3) - \lambda_4 u_2 - \lambda_5 u_3 - 1 \\
\frac{d\lambda_4}{dt} &= -\frac{\partial \mathcal{H}}{\partial R} = \lambda_4\tau_1 - 1 \\
\frac{d\lambda_5}{dt} &= -\frac{\partial \mathcal{H}}{\partial L} = \lambda_5\alpha_2 - \lambda_1\alpha_2
\end{aligned}
$$

with transversality conditions, $\lambda_i(t_f) = 0, i = 1, \dots, 5$. We have that for $0 \le u_i \le 1, i = 1, 2, 3$,

$$\frac{\partial \mathcal{H}}{\partial u_i} = 0, i = 1, 2, 3.$$

That is,

$$
\begin{aligned}
\frac{\partial \mathcal{H}}{\partial u_1} &= B_1 u_1 + \lambda_1\beta U D - \lambda_2\beta U D = 0 \\
&\implies u_1^* = \frac{\beta U D(\lambda_2 - \lambda_1)}{B_1} \\
\frac{\partial \mathcal{H}}{\partial u_2} &= B_2 u_2 - \lambda_3 D + \lambda_4 D = 0 \\
&\implies u_2^* = \frac{D(\lambda_3 - \lambda_4)}{B_2} \\
\frac{\partial \mathcal{H}}{\partial u_3} &= B_3 u_3 - \lambda_3 D + \lambda_5 D = 0 \\
&\implies u_3^* = \frac{D(\lambda_3 - \lambda_5)}{B_3}.
\end{aligned}
$$

Hence, the admissible controls satisfy the optimality conditions,

$$
\begin{aligned}
u_i^* &= \min\left\{ \max\left(\frac{\beta U D(\lambda_2 - \lambda_1)}{B_1} \right), 1 \right\}, \\
u_i^* &= \min\left\{ \max\left(\frac{D(\lambda_3 - \lambda_4)}{B_2} \right), 1 \right\}, \\
u_i^* &= \min\left\{ \max\left(\frac{D(\lambda_3 - \lambda_5)}{B_3} \right), 1 \right\}.
\end{aligned}
$$

These expressions define the optimal intensity of each control strategy at any time t, depending on the current system state and the evolution of the adjoint variables.

Our optimal control formulation extends the dual-control SIS/R framework of Chen and Fan [9], which links macroprudential regulation and easy monetary policy to the effective contagion and recovery rates of credit risk. While their approach establishes the efficiency of dual regulation in a homogeneous credit network, it does not account for behavioural contagion, liquidity feedback, or policy coordination sequencing. In contrast, our optimal control framework extends this approach along two major dimensions. First, we introduce a multi-control structure comprising $u_1(t)$ (deposit insurance intensity), $u_2(t)$ (depositor-calming intervention), and $u_3(t)$ (liquidity injection). This allows the policymaker to target distinct contagion channels, such as solvency perception, behavioural panic, and liquidity constraints, rather than apply a uniform policy. For instance, the deposit insurance control u_1 directly suppresses the effective contact rate between undistressed and distressed banks, while u_2 and u_3 modulate transitions from distress into either insolvency (run) or recovery (liquidity). Our control problem also integrates the feedback between contagion intensity and control cost, capturing endogenous policy responses as contagion evolves. Consequently, our optimal control model generalizes the optimal dual control problem of Chen and Fan [9] to a multi-channel, behaviourally enriched contagion environment that is directly interpretable in terms of real policy tools and institutional mechanisms.

Fig. 4 shows how the basic reproduction number R_0 and its sensitivity change when the parameters vary within plausible ranges. The findings offer clear explanations for the channels that amplify or dampen systemic risk in the banking network. An increase in the recovery rate from exposure (α_1) leads to a steady decline in R_0. When banks are able to restore balance-sheet strength more quickly, the transmission of distress through the system naturally weakens. A similar effect appears in the transition parameters γ_1,

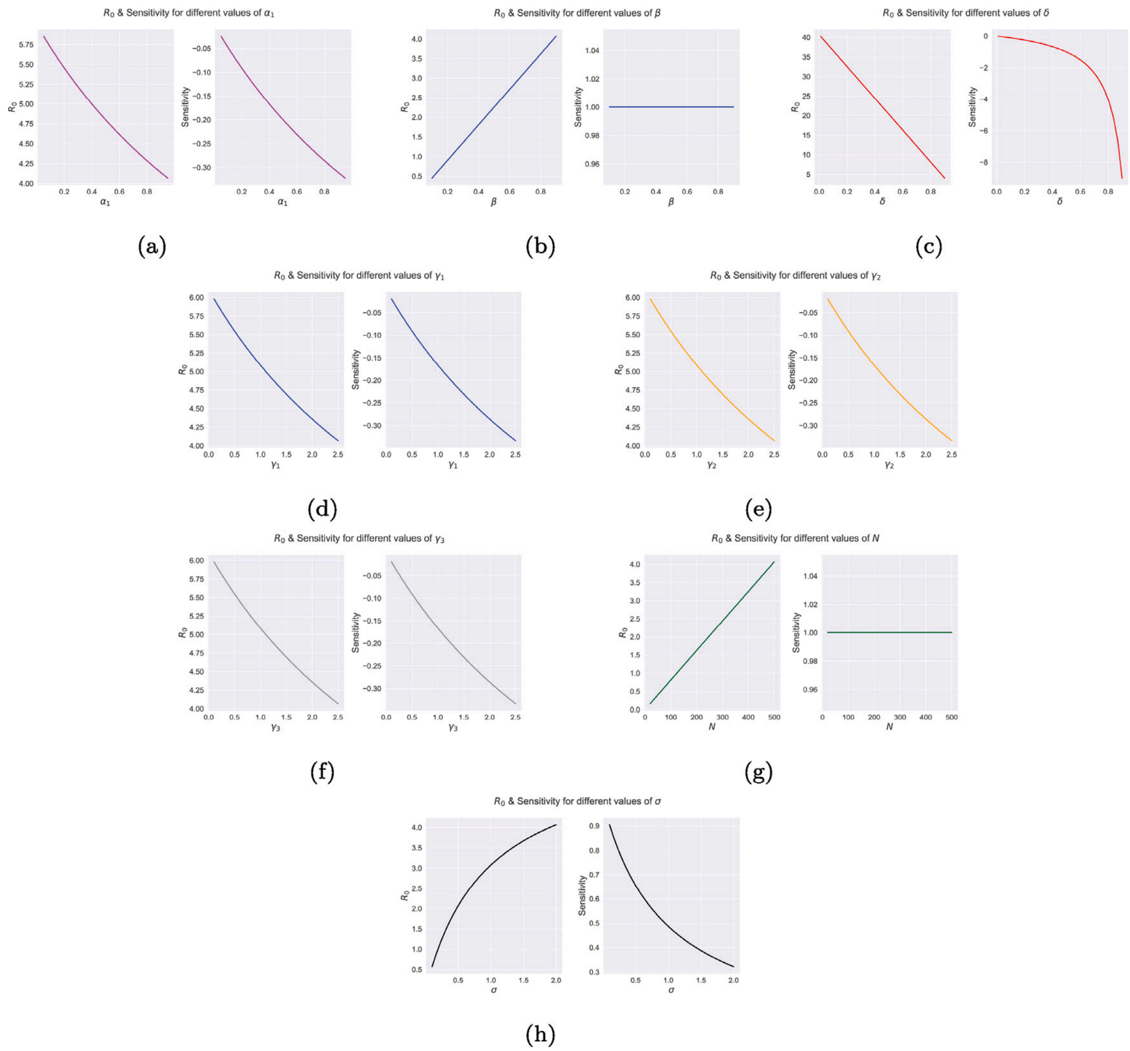

Fig. 4. Sensitivity analysis of R_0 with respect to the model parameters. Each panel illustrates the variation of R_0 (left axis) and its corresponding normalized sensitivity index (right axis) as a single parameter is varied across a plausible range while holding others fixed.

γ_2, and γ_3, which govern movement out of distress, whether into a run state, failure, or the liquid (solvent) state. Faster resolution and recapitalization limit the time banks remain vulnerable, reducing the likelihood of a persistent crisis. In contrast, a rise in the contact rate (β) or the number of interconnected banks (N) increases R_0, reflecting the fact that greater exposure among institutions strengthens contagion channels. The compliance term δ plays a particularly stabilizing role: stronger risk-management effort sharply reduces R_0 and limits the potential for contagion. Finally, the distress-progression rate, σ, acts in the opposite direction when exposures transition to distress more rapidly and shocks travel more easily across the system. The results indicate that the speed of recovery in the banking network, the degree of prudence in risk management, and the level of interbank interconnectedness all affect systemic stability.

4. Numerical simulation

We conduct numerical simulations to assess the effect of the proposed controls on the model. This was done with the GEKKO model of the Python programming language, using the APOPT solver. We set all the weight constants, B_i's, to a constant value of one. That is, all the controls, u_1, u_2, and u_3, were assumed to be of equal significance. We consider an initial scenario in which the system begins with the majority of banks in an undistressed state and a single bank exhibiting signs of distress. The initial conditions are $U = 22, E = 0, D = 1, R = 0, L = 0$, and the parameter values are given in Table 2. The parameter values lie within the empirically and theoretically justified ranges surveyed in seminal studies on network-contagion dynamics [20] and recent empirical quantifications of systemic risk from overlapping balance-sheet exposures [21].

Table 2
Parameter table.

Parameter	Value	Source	Parameter	Value	Source
β	0.4	Estimated	γ_1	0.2	Estimated
δ	0.01	Estimated	γ_2	0.3	Estimated
α_1	0.15	Estimated	γ_3	0.1	Estimated
α_2	0.15	Estimated	τ_1	0.01	Estimated
σ	0.6	Estimated			

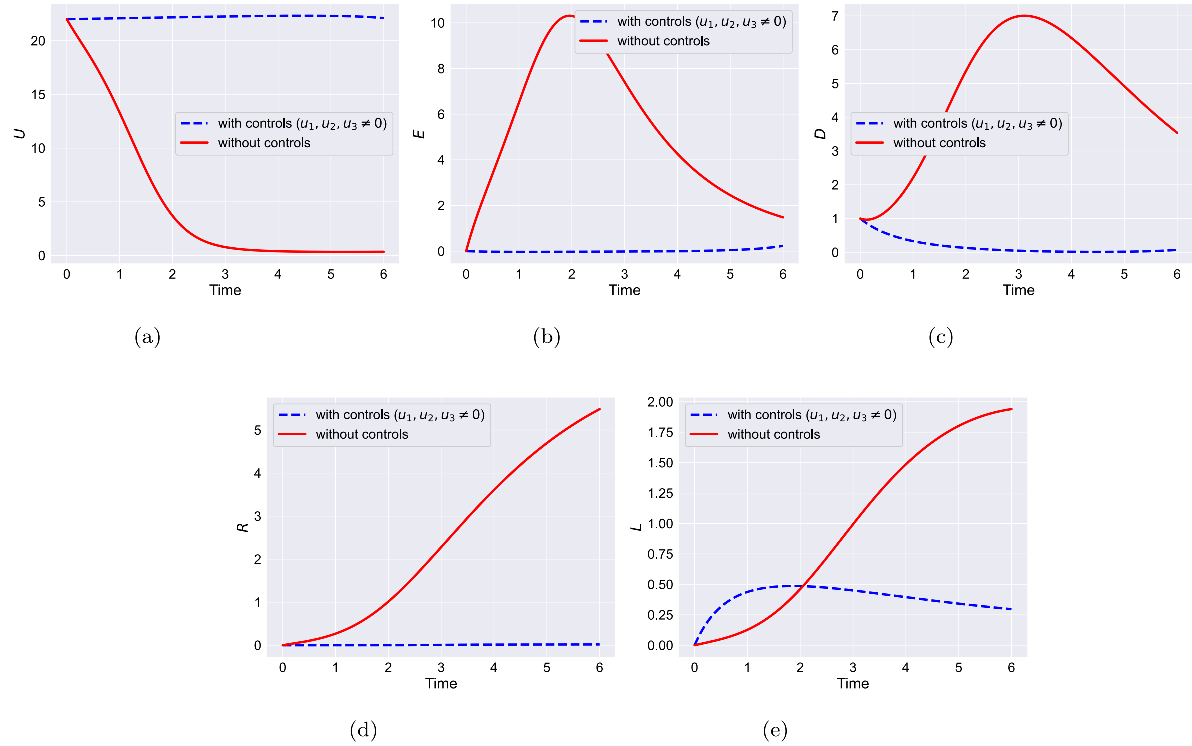

Fig. 5. Plot of the model with (blue dashed) and without (red solid) controls. The blue dashed line indicates the model with controls, and the red solid line represents the model without controls. All three proposed controls were utilized.

In Fig. 5, the plots show the comparison of the model with the proposed controls and the model without the controls. It is observed that implementing all three controls (u_1, u_2, and u_3) has a positive impact on controlling the risk contagion in the banking system. From Fig. 5(a), the model with controls (indicated by dashed blue lines) has an almost straight horizontal line, indicating that the number of undistressed banks is almost constant. Thus there is no risk in the banking system. Fig. 5(b) also shows a very low number of banks in the exposed compartment compared to the graph for the model without controls (represented by the red line). This phenomenon is further explained by Fig. 5(c), where we see that the number of distressed banks starts declining instantaneously. Fig. 5(d) has a zero value for all time when the controls are implemented, indicating that in the presence of the controls, no bank experiences a run state. Lastly, Fig. 5(e) displays the dynamics of the liquid compartment $L(t)$ under both scenarios. In the presence of all three controls, $L(t)$ exhibits a sharp initial increase followed by a gradual decline. This behaviour is consistent with our model's structure: Distressed banks in the D compartment transition to the liquid state via effective risk-management actions ($D \to L$). Thus, when the controls are activated, the rapid reduction in the distressed population (as seen in subplot 5(c)) produces a corresponding surge in $L(t)$ as these banks recover. Once distress has been largely eliminated, however, there are few remaining banks feeding the $D \to L$ transition, and the liquid compartment naturally stabilizes and declines. In contrast, under the no-control scenario, the larger and more persistent distressed population generates a slower but sustained increase in $L(t)$. The behaviour of Fig. 5(e) confirms that the proposed controls effectively suppress contagion, promote rapid recovery, and stabilize the system.

To achieve the desired effect of the controls, the controls must be implemented in a certain way. Fig. 6(a), 6(b) and 6(c) show the exact way of implementing the controls u_1, u_2, and u_3 over time to achieve an optimal state. Fig. 6(a) tells us to start the control u_1 from zero to its maximum value (one in this case) instantaneously at the start of the dynamics, maintain this maximum state of u_1 up to four years, and start reducing the quantity gradually.

To ascertain the contribution of the controls u_2 and u_3, we set the control u_1 to zero. Fig. 7 shows the plots for this scenario. Fig. 7(a) shows a significant reduction in the number of undistressed banks without u_1, indicating that risk propagates in the banking

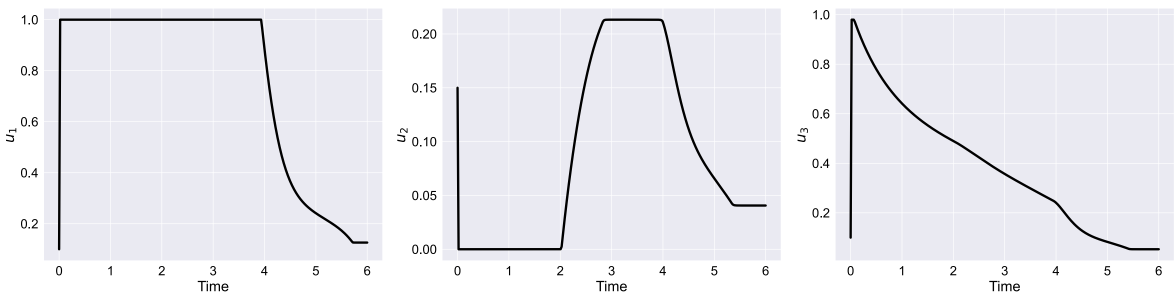

(a) (b) (c)

Fig. 6. Optimal control profiles for deposit insurance (u_1), depositor-calming (u_2), and liquidity injection (u_3). Each curve shows the time-varying intensity of interventions that minimize systemic risk under the optimal control framework.

system; however, this scenario is slightly better than the case where no controls are implemented. The exposed compartment shows a significant increase in number before it starts to decline, as shown in Fig. 7(b). A key observation is that the number of banks decreases more slowly with controls than without. This indicates that banks in this compartment tend to remain in the exposed state for a longer duration when only u_2 and u_3 are implemented, before either becoming fully distressed or recovering (returning to an undistressed state). As indicated earlier, Fig. 7(c) shows an increase in the number of distressed banks, but it is relatively low compared to the case where no controls are implemented. In Fig. 7(d), we can still see that for the controlled population, no banks experience the run state. This is because we are implementing the control u_2, which significantly reduces the number of banks moving to the run compartment. Fig. 7(e) shows a substantial rise in the liquid compartment $L(t)$ relative to the no-control case. This behaviour is consistent with the model dynamics: under the control pair (u_2, u_3), a large fraction of banks that become distressed are able to regain solvency and transition into the liquid state via the $D \to L$ mechanism. Liquidity support from u_2 improves balance-sheet resilience, while depositor-calming actions under u_3 suppress further deterioration, ensuring that distressed banks recover rather than remaining trapped in the D or R compartments. As a consequence, the liquid compartment grows rapidly under (u_2, u_3), reflecting the effectiveness of these controls in stabilizing the system even in the absence of deposit insurance. In Fig. 8, we present the visual representation of how the control must be applied to achieve an optimal state.

Lastly, we evaluate the significance of the control u_1 by setting the other control variables (u_2 and u_3) to zero. The results, as demonstrated by Fig. 9, are that u_1 is very efficient. That is, by only implementing the control u_1, we can significantly reduce the contagion in the banking system. This is consistent with what was observed by the Federal Deposit Insurance Corporation [22]. In Fig. 10, we have the visual representation of how the control must be applied.

The robustness experiment with one and two banks initially in the exposed and distressed compartments, respectively, confirms the importance of early deposit-insurance coverage (see Fig. 11). Implementing all three controls (u_1, u_2, u_3) produces the strongest stabilization, while deposit insurance u_1 on its own continues to deliver a sharp reduction in both exposure and distress, preventing the amplification of shocks and suppressing runs throughout the horizon. Because u_1 is comparatively less costly to implement than liquidity injections or depositor-calming measures, it remains the most cost-effective single-instrument intervention. In contrast, the $(u_2 + u_3)$ combination is more effective as a reactive, post-contagion stabilization mechanism, facilitating rapid resolution once banks have become distressed, but is less successful than u_1 at preventing the initial propagation of shocks. Thus, even under a more adverse initial condition, early deposit-insurance coverage plays a central preventive role, while u_2 and u_3 remain valuable but costlier tools that are best deployed after contagion has already begun.

4.1. Policy relevance: Insights from the SVB 2023 run

We briefly relate the model to the 2023 failure of Silicon Valley Bank (SVB) to show its practical relevance. The episode is a clear illustration of how distress can spread quickly once information circulates and depositor confidence deteriorates. In terms of our six-compartment structure, SVB can be viewed as moving from the Exposed (E) state, reflecting mounting losses on long-duration assets and visible balance-sheet strain into the Distressed (D) state as liquidity pressures grew and large withdrawals by venture-capital clients accelerated. The subsequent "digital run", coordinated through online communication channels, corresponds to the Run (R) compartment, where depositors acted almost simultaneously and overwhelmed the bank's liquidity buffer. A stronger deposit-insurance (u_1) could have tempered fears of depositor loss, while a clear supervisory communication or temporary withdrawal management (u_2) might have softened the momentum of withdrawals. Similarly, a timely liquidity injection (u_3) like the Federal Reserve's emergency facility, could have supported a quicker shift from the Distressed to the Liquid compartment and reduced the risk of broader spillovers. This demonstrates that the proposed optimal control model not only offers a rigorous theoretical structure for analysing systemic risk but also provides a policy-relevant perspective for understanding and mitigating contemporary crises such as the SVB 2023 run.

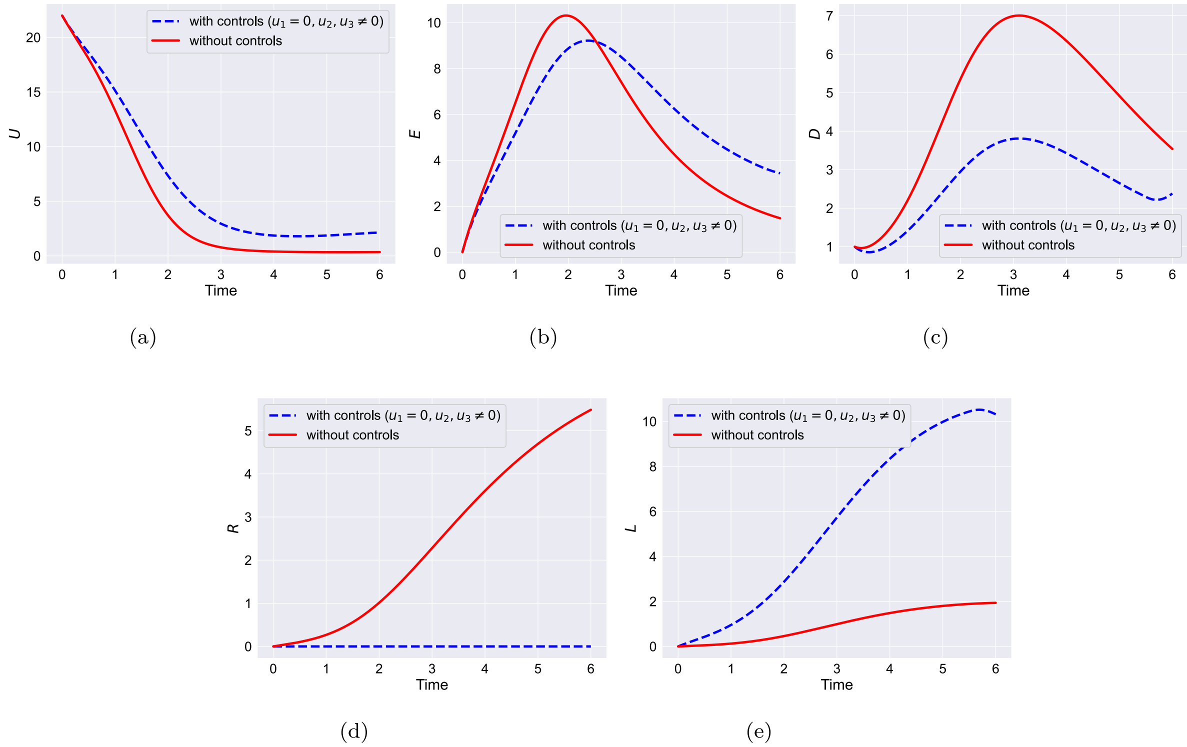

Fig. 7. System dynamics with $u_1 = 0$; controls u_2 and u_3 mitigate distress and prevent runs. The blue dashed line is the model with control, and the red solid line is the model without control.

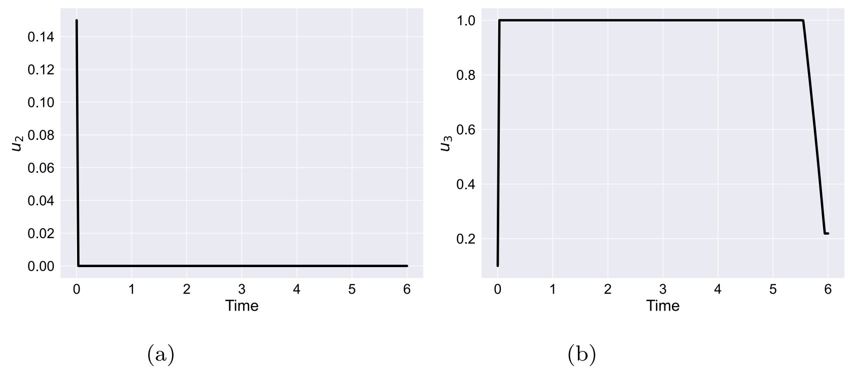

Fig. 8. Optimal control profiles for u_2 (depositor-calming) and u_3 (liquidity injection) over time.

5. Conclusion and recommendations

We develop an epidemiologically inspired framework for analysing financial contagion within banking systems, borrowing concepts from compartmental models used in infectious disease research. The banking network is divided into six states (undistressed, exposed, distressed, run, failed, and liquid) which together capture the nonlinear movements of risk driven by interbank linkages and depositor reactions. Within this structure, we establish fundamental properties of the model, including boundedness, positivity of solutions, and the presence of two equilibrium points: a risk-free equilibrium, where all institutions remain sound, and a risk-persistent equilibrium, where distress continues at manageable levels. The shift between these states depends on the basic reproduction number $\mathcal{R}_0$, which summarizes the underlying contagion mechanisms and provides a threshold for stability. Sensitivity analysis shows how parameters such as the compliance level δ, contact rate β, and the transition rates γ_i influence the evolution of systemic stress. To counter the spread of distress, we introduce a set of policy controls (deposit insurance, depositor-calming measures, and liquidity support) and determine their optimal time paths using Pontryagin's Maximum Principle. The numerical experiments illustrate how each control mechanism helps limit the spread of risk within the banking system, with deposit insurance

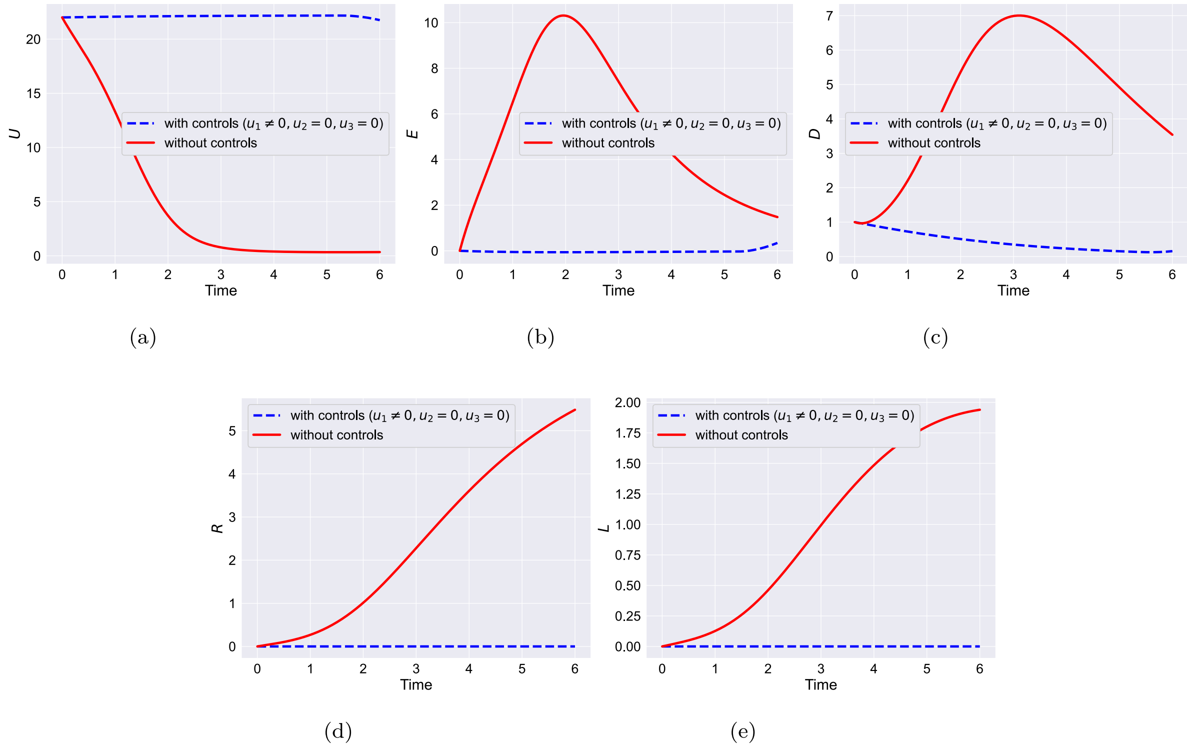

Fig. 9. Effect of the deposit insurance control (u_1) on contagion dynamics. Blue dashed line shows the controlled case; red solid line shows the uncontrolled case.

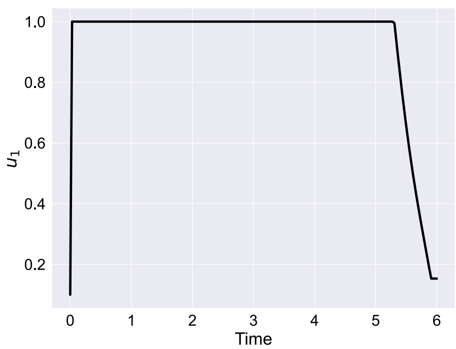

(a)

Fig. 10. Optimal control profile for deposit insurance (u_1) over time.

proving especially effective at the onset of distress. By following both the evolution of contagion and the effects of timely policy responses, the optimal control policy offers regulators a practical way to interpret, and potentially manage, modern bank-run episodes.

It is important to acknowledge that the present model is deterministic and does not incorporate random liquidity shocks or behavioural feedback which is capable of amplifying or dampening systemic stress. Further research could include reformulating compartmental dynamics as a system of stochastic differential equations to include exogenous liquidity and solvency shocks and studying how such unpredictability affects the optimal control. The model could also be extended to account for heterogeneous banking networks, stochastic shocks, or incorporating behavioural feedback from depositors and markets.

Consent for publication

All authors consent to the publication of this research

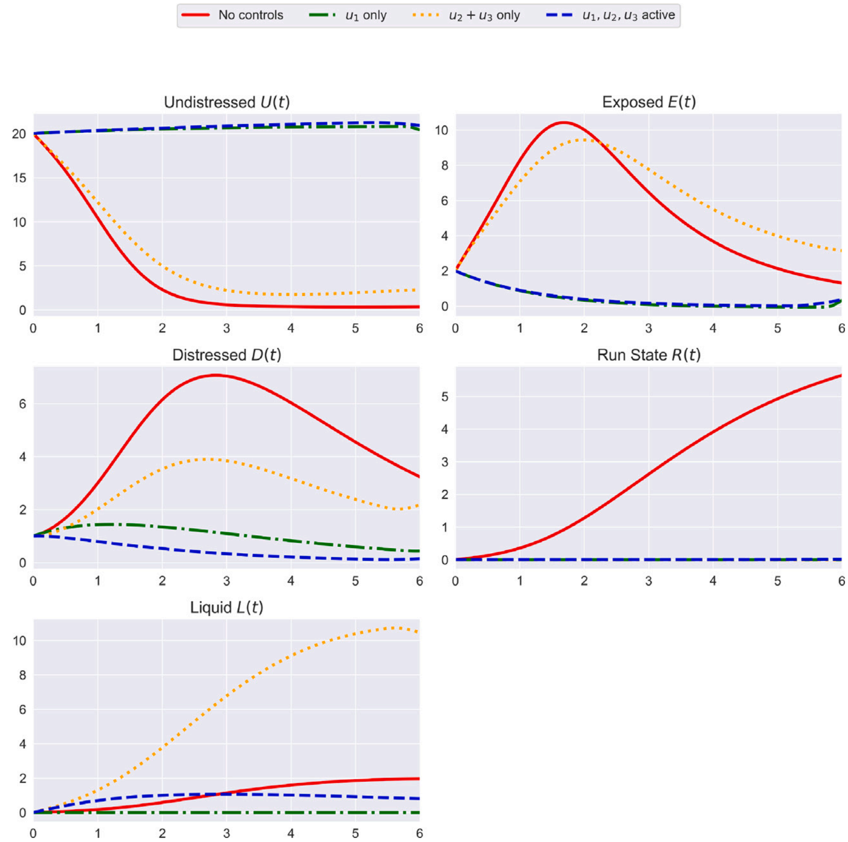

Fig. 11. Robustness check with one initially distressed banks and two exposed banks. The three controls (u_1, u_2, u_3) provide the strongest stabilization, while deposit insurance u_1 alone remains an effective and low-cost preventive tool for suppressing early contagion. The $(u_2 + u_3)$ combination supports post-distress resolution but is less effective at preventing amplification, confirming that the main conclusions of the baseline analysis remain robust.

CRediT authorship contribution statement

Samuel Asante Gyamerah: Writing – review & editing, Writing – original draft, Software, Methodology, Funding acquisition, Formal analysis, Conceptualization. **Emmanuel Afrifa:** Writing – original draft, Software, Methodology, Formal analysis, Conceptualization. **Perpetual Andam Boiquaye:** Writing – review & editing, Writing – original draft, Methodology, Formal analysis, Conceptualization. **Nelson Dzupire:** Writing – review & editing, Writing – original draft, Methodology, Conceptualization.

Funding

The first author acknowledges the start-up research grant from Toronto Metropolitan University, Toronto, Canada.

Declaration of competing interest

The authors declare no conflict of interest.

Data availability

No data was used in this work.

References

[1] N. Chen, H. Fan, Credit risk contagion and optimal dual control—An SIS/R model, Math. Comput. Simulation 210 (2023) 448–472.
[2] M. Raddant, D.Y. Kenett, Interconnectedness in the global financial market, J. Int. Money Financ. 110 (2021) 102280.
[3] A. Sogani, The great lockdown vs. The great depression and the 2008 global financial crisis, E-International Relations 2 (2020).
[4] A. Metrick, The failure of silicon valley bank and the panic of 2023, J. Econ. Perspect. 38 (1) (2024) 133–152.
[5] M. Akhtaruzzaman, S. Boubaker, J.W. Goodell, Did the collapse of silicon valley bank catalyze financial contagion? Financ. Res. Lett. 56 (2023) 104082.
[6] X. Liu, A model of systemic bank runs, J. Financ. 78 (2) (2023) 731–793.
[7] J. Peck, A. Setayesh, Bank runs and the optimality of limited banking, Rev. Econ. Dyn. 47 (2023) 100–110.
[8] G. Brandi, R. Di Clemente, G. Cimini, Epidemics of liquidity shortages in interbank markets, Phys. A 507 (2018) 255–267.
[9] N. Chen, H. Fan, Contagion and supervision of liquidity crisis in interbank markets: Based on the SIS network model, Phys. A 629 (2023) 129216.
[10] I. Irakoze, D. Ikpe, F. Nahayo, S.A. Gyamerah, Time dynamics of systemic risk in banking networks: A UEDR-pde approach, AppliedMath 5 (2) (2025) 54.
[11] I. Irakoze, F. Nahayo, D. Ikpe, S.A. Gyamerah, F. Viens, Mathematical modeling and stability analysis of systemic risk in the banking ecosystem, J. Appl. Math. 2023 (1) (2023) 5628621.
[12] J.P. Sabourin, Rethinking the role of deposit insurance: Lessons from the recent financial crisis, in: Financial Crisis Management and Bank Resolution, Informa Law from Routledge, 2020, pp. 133–138.
[13] V. Sardana, S. Singhania, Insuring deposits, ensuring stability: A critical evaluation of six decades of deposit insurance in the Indian banking sector, J. Risk Manag. Financ. Institutions 17 (2) (2024) 197–212.
[14] N. Alam, G. Sivarajah, M.I. Bhatti, Do deposit insurance systems promote banking stability? Int. J. Financ. Stud. 9 (3) (2021) 52.
[15] A. Adom-Konadu, A.L. Sackitey, M. Anokye, Local stability analysis of epidemic models using a corollary of gershgorin's circle theorem, 2022.
[16] D. Bejarano, E. Ibargüen-Mondragón, E.A. Gómez-Hernández, A stability test for non linear systems of ordinary differential equations based on the gershgorin circles, Contemp. Eng. Sci. 11 (91) (2018) 4541–4548.
[17] O. Sharomi, T. Malik, Optimal control in epidemiology, Ann. Oper. Res. 251 (2017) 55–71.
[18] J.K.K. Asamoah, B. Safianu, E. Afrifa, B. Obeng, B. Seidu, F.A. Wireko, G.-Q. Sun, Optimal control dynamics of gonorrhea in a structured population, Heliyon 9 (10) (2023).
[19] E.C. Chukukere, A. Omame, C. Onyenegecha, S. Inyama, Mathematical analysis of a model for chlamydia and gonorrhea codynamics with optimal control, Results Phys. 27 (2021) 104566.
[20] P. Glasserman, H.P. Young, How likely is contagion in financial networks? J. Bank. Financ. 50 (2015) 383–399.
[21] S. Poledna, S. Martínez-Jaramillo, F. Caccioli, S. Thurner, Quantification of systemic risk from overlapping portfolios in the financial system, J. Financ. Stab. 52 (2021) 100808.
[22] Federal Deposit Insurance Corporation, Remarks by FDIC chairman martin j. Gruenberg on the financial stability oversight council report, 2023, https://www.fdic.gov/news/speeches/2023/spsept2823.html. (Accessed 26 October 2024).